Eur. Phys. J. B **54**, 225–241 (2006)
DOI: 10.1140/epjb/e2006-00443-y

THE EUROPEAN PHYSICAL JOURNAL B

# Optics of embedded semiconductor nano-objects using a hybrid model: bare versus dressed polarizabilities

C.M.J. Wijers[a], J.-H. Chu, and O. Voskoboynikov

Department of Electronics Engineering and Institute of Electronics, National Chiao Tung University, 1001 Ta Hsueh Rd., Hsinchu 300, Taiwan

Received 16 June 2006 / Received in final form 2 November 2006
Published online 22 December 2006 – 

**Abstract.** The influence of the surrounding semiconducting matrix upon the optical response of embedded nano-objects (quantum dots) has been investigated. This system can be described by means of a hybrid model, where the full response is a combination of a macroscopic electrostatic response term and a dynamic response term, obtained quantum mechanically. The result is a modified discrete dipole model, where excess discrete dipoles having an excess polarizability with respect to a uniform background identical to the dielectric host material represent the response. In this model all electrodynamic interactions are screened by the host material. The electrostatic response is obtained by approximating the quantum dots by embedded dielectric oblate ellipsoids. Closed expressions for the electrostatic response of these ellipsoids have been derived. The electrodynamic nature of the dynamic quantum mechanical polarizability term however is unclear. It is not certain whether this polarizability is dressed or bare. Therefore we have investigated in detail the consequences of both options. Although there is no real qualitative difference between them, the difference is so large that experiment can easily discriminate between both. Results should be easily measurable anyhow.

**PACS.** 41.20.Cv Electrostatics; Poisson and Laplace equations, boundary-value problems – 78.30.Fs III-V and II-VI semiconductors – 78.67.-n Optical properties of low-dimensional, mesoscopic, and nanoscale materials and structures

## 1 Introduction

When devices are made out from semiconductors it is essential to know whether these semiconductors are direct or indirect gap ones. Only direct gap semiconductors allow for direct interaction between light and the charges (electrons/holes) of the semiconductor. This property in turn determines what kind of devices or construction elements can be made from these semiconductors. The most recent class of semiconductor building blocks are nano-objects like quantum dots and nano-rings. They are most promising in the field of new optical applications, but as yet there are not really usable models to describe their linear collective optical behavior. Optics in combination with nano-objects relies either upon expressions for optical absorption [1] or upon oscillator strengths [2,3], being the squared modulus of the optical transition matrix element [4]. Here we investigate how the hybrid model (introduced by us before [5–7] to treat the linear optical properties of free floating semiconducting nanosized objects) has to be extended to account for the influence of embedding in a foreign semiconducting host material. We consider a metamaterial built from nano-objects of characteristic size $a$, occupying a rectangular lattice with lattice constant $a_L$. The hybrid character of the model relates to the fact that it describes the electrodynamic response as a combination of a local macroscopic continuum description for the static and a nonlocal discrete description for the dynamic part of the response.

In this paper we investigate two aspects of this hybrid model, both of them related to and essential for the understanding of the optics of embedded nano-objects. The first aspect concerns the dynamic part of the polarizability. This dynamic part of the hybrid model is a quantum mechanical polarizability term where only a few pairs of quantum states near the absorption edge play a role. To combine it properly with the static part of electrodynamic origin we have to know its electromagnetic nature in the sense whether this quantum mechanical term is defined with respect to the average internal or with respect to the external electric field. The first option classifies the polarizability as bare and the second as dressed.

The second aspect concerns the static part of the optical response problem. Although it is best resolved in a traditional macroscopic local way, a reformulation of the results in a nonlocal discrete way improves both the physical insight and the connection to the dynamic quantum

[a] e-mail: wijers@faculty.nctu.edu.tw

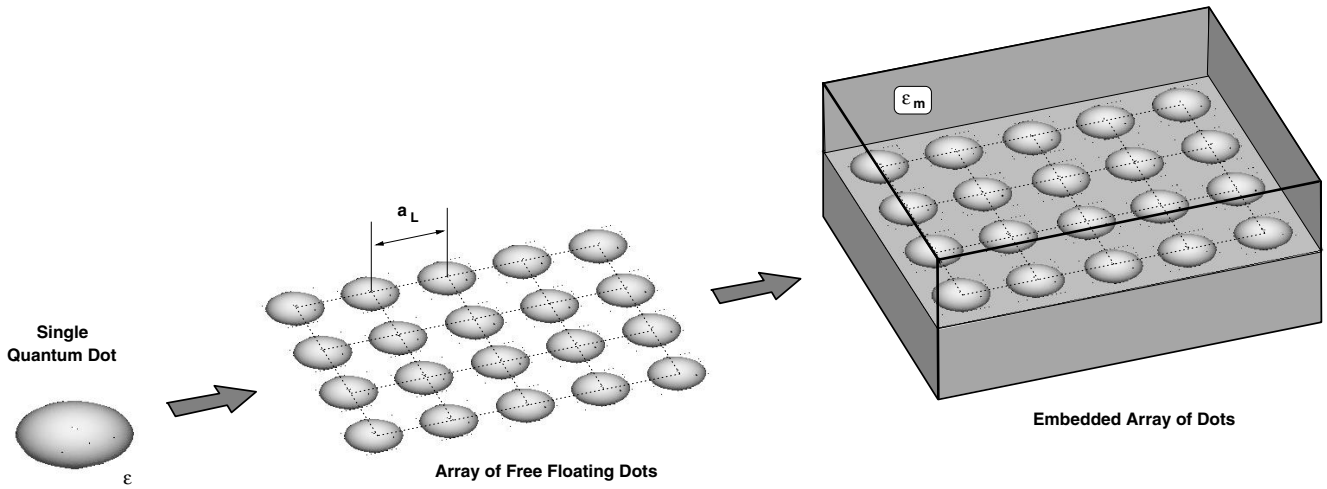


**Fig. 1.** Conceptual picture of the building of a metamaterial from semiconductor nano-objects (embedded ellipsoidal quantum dots).

mechanical part of the description. It turns out to be very beneficial to introduce the concepts of field penetration and excess polarization. Field penetration simply means the fraction of the external field which manages to enter the nano-object and excess polarization means that only part of the polarization density determines the optical response of the nano-object.

It is not easy to distinguish immediately effects caused by embedding, often taken to be equivalent to screening, and effects related to the bare/dressed picture. Yet they are not the same. A free floating nano-object e.g. has different bare and dressed polarizabilities. On the other hand the bare (full) polarizability of a nano-object will not change upon embedding.

After the reformulation of all results, both the dynamic quantum mechanical and static local, in terms of the same nonlocal discrete description, an ensemble of these nano-objects can effectively be treated by means of modified discrete dipole theory. The response of an embedded dielectric ellipsoidal nano-object is used for the electrostatic part in order to model as closely as possible realistic semiconductor quantum dots. We combine this discrete nonlocal description for the excess response of the dots with a local continuum description for the uniform background, extending over the host material, including the dots. Since there is no general consensus whether the dynamic quantum mechanical part of the polarizability is bare or dressed, this paper will investigate the consequences of either choice. Temperature dependence will not be taken into account, ($T = 0$ K situation), but partly temperature dependence will be accounted for by using a damping term $\gamma$ in the dynamical part.

## 2 Theory

In this section we will derive the hybrid model and use it to describe the optical response of metamaterials composed of nano-objects like quantum dots, embedded in a dielectric host material (see Fig. 1). The nano-objects will be assumed in this paper to have a static (low frequency) dielectric constant $\epsilon$ different from the dielectric constant $\epsilon_m$ of the host material. Both the host material and the nano-objects at low frequencies will be assumed to be transparent, in other words $\epsilon_m$ and $\epsilon$ are supposed to be real. Only the dynamical part $\Delta\alpha(\omega)$ has a nonzero imaginary component, due to the complex character of $f_{hl,el}(\omega)$. These assumptions reflect accurately the behavior of the dots in the frequency range near the interband transitions onset.

### 2.1 Bare and dressed polarizabilities of semiconductor nano-objects

The polarizability of a nano-object determines how large the dipole moment of that object as induced by an electric field, will be [5]. Hence this electric field needs to be specified in order to define properly the polarizability. It may look at first glance that this could not be much of a problem, but actually this point in general is not well taken. Although, once a choice has been made, the situation is further clear, often this choice has been left in the open and uncertainty is the result. In fact two choices of electric field can be equally well defended as a proper polarizability reference. At first it is logical that the electrons (and holes) which determine ultimately the polarizability, react locally and that means that they will react upon the internal electric field (local means here dependent upon electric fields *inside* the nano-object). A polarizability defined with respect to the internal electric field is a *bare polarizability*. Any experimentalist however will correctly object that such a choice is not practical, since there is no way to measure this internal field. Therefore to define the polarizability with respect to the external electric field is also a result of common sense, although such field can only be measured at the furthest place of any electron or hole in the nano-object. A polarizability defined with respect to the external

electric field is a *dressed polarizability* and that is where experimental values refer to.

To define the polarizability $\alpha$ for a given nano-object we have to introduce first the *dipole strength* $\mathbf{p}$:

$$\mathbf{p} = \int_V d\mathbf{r}' \, \mathbf{P}(\mathbf{r}') \tag{1}$$

where $\mathbf{P}(\mathbf{r})$ is the polarization density and $V$ the volume of the nano-object. The bare polarizability $\alpha_B$ is defined with respect to the internal electric field $\mathbf{E}_I$ by:

$$\mathbf{p} = \overleftrightarrow{\alpha}_B \, \mathbf{E}_I. \tag{2}$$

This electric field $\mathbf{E}_I$ is a macroscopic field and is therefore a spatial average of the microscopic electric field $\mathbf{e}(\mathbf{r})$. The dressed polarizability $\alpha_D$ is defined by:

$$\mathbf{p} = \overleftrightarrow{\alpha}_D \, \mathbf{E}_X \tag{3}$$

where $\mathbf{E}_X$ is the external electric field in the case of a single nano-object. The above definitions are only meaningful for ellipsoidal bodies with a constant internal field and represent the local macroscopic continuum description. For the nonlocal discrete description we need the definition:

$$\begin{aligned} \mathbf{p} &= \overleftrightarrow{\alpha}_B \, \mathbf{E}_A \\ \mathbf{E}_A &= \mathbf{E}_X + \overleftrightarrow{\mathbf{t}} \, \mathbf{p} \end{aligned} \tag{4}$$

where $\mathbf{E}_A$ is the applied electric field (definition) and $\mathbf{t}$ is the full electromagnetic selfinteraction tensor for the nano-object, to be called further *intracellular transfer tensor*. For dielectric spheres or ellipsoids, the applied field equals statically the internal field. Therefore, at least for this paper, the bare polarizability remains the same. It is easy to show the following elementary relationship between the two kinds of polarizability [6]:

$$\overleftrightarrow{\alpha}_D^{-1} = \overleftrightarrow{\alpha}_B^{-1} - \overleftrightarrow{\mathbf{t}} \, . \tag{5}$$

When more nano-objects are present the external field $\mathbf{E}_X$ needs to be replaced by the local field $\mathbf{E}_L$ in all expressions above. The distinction between bare and dressed polarizabilities is necessary to understand properly the physics behind the hybrid method, as will be worked out in the rest of this paper.

### 2.2 Addition of dynamical part polarizability

In the hybrid model we have to add a static electromagnetic and a dynamic quantum mechanical polarizability. It is obvious that only polarizabilities of the same kind, dressed or bare, can be added in a meaningful way. This is no problem for the static electromagnetic part, since this will be derived unambiguously as a *dressed* polarizability as we will show in the next section. For the dynamic part of the polarizability, the quantum mechanical part, the situation is different. In a previous publication [6] we have shown already that the polarizability of a nano-object for photon frequencies near the energy gap of the semiconductor the object is made from, can be approximated by the sum of a static polarizability and the dynamical contribution $\Delta\alpha(\omega)$, given by:

$$\begin{aligned} \Delta\alpha(\omega) = \frac{3}{4} \, \frac{e^2}{\hbar} \, r_{eh}^2 \left[ \hat{\mathbf{x}}\hat{\mathbf{x}}^T + \hat{\mathbf{y}}\hat{\mathbf{y}}^T \right] \\ \times \sum_{l=0}^{-2} \left| \langle F_{hl} | F_{el} \rangle_V \right|^2 f_{hl,el}(\omega) \end{aligned} \tag{6}$$

where $r_{eh}$ is the matrix element of the spatial coordinate $\mathbf{r}$ between states $e$ (electron) and $h$ (hole) over the bulk unit cell $V_B$. $\langle F_{hl} | F_{el} \rangle_V$ is the overlap matrix element between envelope functions of index $l$ for hole and electron over the volume $V$ of the nano-object. $f_{hl,el}(\omega)$ is a complex frequency dependent function. Direct vector products $\hat{\mathbf{x}}\hat{\mathbf{x}}^T, \hat{\mathbf{y}}\hat{\mathbf{y}}^T$ indicate the $x$- and $y$-position on the diagonal of the polarizability tensor.

We have to combine this $\Delta\alpha(\omega)$ properly with the static dressed polarizability $\alpha_D$. Then we have to know whether equation (6) represents a bare or a dressed polarizability. To answer that question we reformulate the one-particle Hamiltonian as given in [5], equation (14):

$$\begin{aligned} H &= H_0 + H_1(\mathbf{r}, t) \\ H_1(\mathbf{r}, t) &= -\frac{q}{2m} \left[ \mathbf{p}^T \mathbf{A}(\mathbf{r}, t) + \mathbf{A}^T(\mathbf{r}, t) \mathbf{p} \right] \end{aligned} \tag{7}$$

where $H_1(\mathbf{r}, t)$ is the time dependent perturbation, split in [5] into $\hat{H}_D$, a dissipative part, and the actual perturbation $W(\mathbf{r})$. If the $\mathbf{A}(\mathbf{r}, t)$ would have been known exactly, solution of the problem would have been straightforward and any further discussion would have been superfluous. This however is not the case and approximations have to be made to arrive at a practical solution. The only way to proceed from here towards a traditional expression for the polarizability as given e.g. in equations (2, 3) is by introducing an auxiliary vector potential $\mathbf{A}_U(t)$ being constant over the volume of the nano-object:

$$\begin{aligned} \mathbf{A}(\mathbf{r}, t) &= \Delta\mathbf{A}(\mathbf{r}, t) + \mathbf{A}_U(t) \\ \Delta\mathbf{A}(\mathbf{r}, t) &= \mathbf{A}(\mathbf{r}, t) - \mathbf{A}_U(t). \end{aligned} \tag{8}$$

Then we can continue as in [5] and replace there $\mathbf{A}_I$ by $\Delta\mathbf{A}$ and use $\mathbf{A}_U$ to define $W(\mathbf{r})$. It is from the matrix element of $W$, that this constant $\mathbf{A}_U$ has to be taken out to arrive at a proper polarizability. The crucial step in this essentially approximative procedure is the choice of $\mathbf{A}_U$. The first choice is $\mathbf{A}_U = \mathbf{A}_X$, as has been done in [9] and correspondingly in [5]. With this assignment the resulting polarizability will be dressed. The other common choice is to use the spatial average of the vector potential $\langle \mathbf{A} \rangle$ and this choice would yield a bare polarizability. At present there is a definite preference for this option since it accounts better for the contribution of the sources inside

the nano-object. Yet such argument is purely electromagnetic and does not account for effects of quantum mechanical nonlocality, which in general weaken these short range electromagnetic interactions. As yet there is no strong evidence which of the two approximations is the best. The interested reader can find additional information about this important subject in references [8,9] about the origin of the debate, in references [10–12] about the modern formulation and in references [13–17] about more recent use of a quantum mechanically derived polarizability.

All of this brings us to the conclusion that it has not been agreed upon whether quantum mechanical expressions for the polarizability of dielectric bodies (sum over states expressions) are bare or dressed. Yet it is clear that especially a hybrid model needs to find a way to deal with this ambiguity. Definitely we have a clear preference for the bare option, but it is not the aim of this paper to resolve this longstanding bare/dressed ambiguity here. Instead we will investigate both options, the one where we add $\Delta\alpha(\omega)$ to the bare and the one where we add it to the dressed polarizability and analyze the results for both cases. It will depend on the outcome of experiments to decide which option is the better one. At forehand we mention that we will use both for the theory and for the calculations, the bare polarizability as the main (internal) carrier of information, as will be explained further on.

For the first option, adding to the static bare polarizability, we have to realize that this polarizability is obtained as a dressed one, $\alpha_D$, so we have to convert it first to a bare one, $\alpha_B$, using (5):

$$\alpha_B = \left[\alpha_D^{-1} + t\right]^{-1}. \tag{9}$$

Then we can add the dynamical part $\Delta\alpha(\omega)$ to this static bare polarizability $\alpha_B$:

$$\alpha_B(\omega) = \alpha_B + \Delta\alpha(\omega) \tag{10}$$

where $\alpha_B(\omega)$ is the dynamic bare polarizability.

The other option is to add $\Delta\alpha(\omega)$ to the static dressed polarizability $\alpha_D$. This can be done straightaway:

$$\alpha_D(\omega) = \alpha_D + \Delta\alpha(\omega) \tag{11}$$

where $\alpha_D(\omega)$ is the dynamic dressed polarizability. However, when we add the dynamical part $\Delta\alpha(\omega)$ to the dressed polarizability, we have to convert the result to a corresponding bare polarizability. To that end we use again (5)

$$\alpha_B(\omega) = \left[\alpha_D^{-1}(\omega) + t\right]^{-1}. \tag{12}$$

Notice that we have returned to a scalar description, but since all tensors involved are diagonal, this is possible and improves reading. Both options, (10) and (12), are shown as a diagram in Figure 2.

Here the bare polarizability $\alpha_B(\omega)$ is the full bare polarizability of the nano-object, different from the excess bare polarizability, to be used later. The full bare polarizability is an intrinsic property of the nano-object not dependent on or influenced by embedding. Explicit expressions for the basic parameters $\alpha_D$ and $t$ will be given in Section 2.4. If we choose the bare option for the quantum mechanical part, we will refer to the bare polarizability $\alpha_B(\omega)$ given by (10) as *added to bare polarizability* and if we choose a dressed quantum mechanical part, we refer to the bare polarizability $\alpha_B(\omega)$ given by (12) as *added to dressed polarizability.*

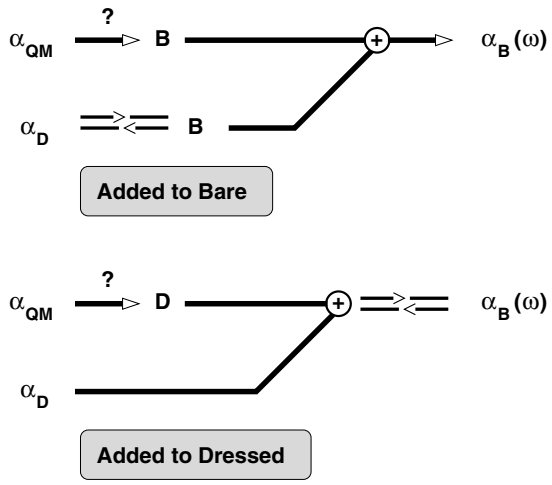


**Fig. 2.** Addition of Dynamical part: Added to bare (B) versus added to dressed (D). Double arrows point to bare/dressed conversion.

### 2.3 Embedded dielectric objects: electric fields

In the hybrid model we need the static polarizability of the nano-object, for which we use the approximation here of an ellipsoidal dielectric body. This oblate ellipsoid has short axis $c$ and long axis $a$ as treated in [6]. We will use again $\zeta = c/a$. For the transformation to elliptic coordinates we use:

$$\begin{aligned} x &= f\ \cosh\xi\ \cos\eta\ \cos\phi \\ y &= f\ \cosh\xi\ \cos\eta\ \sin\phi \\ z &= f\ \sinh\xi\ \sin\eta \end{aligned} \tag{13}$$

where $f = \sqrt{a^2 - c^2}$. A dielectric ellipsoid embedded in a different dielectric medium obeys the macroscopic version of the Poisson equation:

$$\nabla \cdot \mathbf{D} = 0$$

where $\mathbf{D} = \varepsilon\,\epsilon_0\mathbf{E}$ is the dielectric displacement and $\varepsilon$ the dielectric constant. This allows for the introduction of the electrostatic potential $\Phi(\mathbf{r})$ in the usual way and because of the cylindrical symmetry of the problem we have to solve the following Poisson equation for $\Phi(\mathbf{r})$:

$$\left[\frac{\partial^2}{\partial\xi^2} + \tanh\xi\frac{\partial}{\partial\xi} + \frac{\partial^2}{d\eta^2} - \tan\eta\frac{\partial}{\partial\eta}\right]\Phi = 0. \tag{14}$$

This differential equation can be solved by separation of coordinates:

$$\Phi(\eta,\xi,\phi) = G(\eta)\,F(\xi). \tag{15}$$

It suffices to use only the following $\eta$-dependence:

$$G_0(\eta) = -E_0 f \sin\eta \tag{16}$$

where $E_0$ is the amplitude of the externally applied uniform electric field $\mathbf{E}_X = E_0\hat{\mathbf{z}}$. For the solution $F(\xi)$ connected to this $\eta$-dependence, we need the following two independent solutions:

$$\begin{aligned} F_0(\xi) &= \sinh\xi \\ F_1(\xi) &= 1 \,-\, \sinh\xi\, \tan^{-1}\left(\frac{1}{\sinh\xi}\right). \end{aligned} \tag{17}$$

Since the condition $\xi = \xi_0$ establishes the surface of the oblate ellipsoid, varying $\phi,\eta$ means scanning this surface. For later use we need the expression for the external potential $\Phi_X(\mathbf{r})$:

$$\Phi_X(\mathbf{r}) = -E_0\, z \;=\; G_0(\eta)\,F_0(\xi). \tag{18}$$

Freezing the $\eta$-dependence to $G(\eta) = G_0(\eta)$, reduces the dielectric oblate ellipsoid problem to a one-dimensional problem in the functions $F_0(\xi)$ and $F_1(\xi)$. So we write the electrostatic potential $\Phi(\mathbf{r})$ as:

$$\Phi_v(\xi,\eta,\phi) = G_0(\eta)\;[A_v F_0(\xi) + B_v F_1(\xi)] \tag{19}$$

where the index $v$ equals $I$ for the inner and $O$ for the outer region of the ellipsoid, making 4 unknowns in total. Two of the unknowns can be eliminated by requiring that the electric field inside is constant and that the electric field outside for large $\xi$ has to coincide with the external field $\mathbf{E}_X$. As a result $B_I = 0$ and $A_O = 1$. The remaining coefficients $A_I, B_O$ follow from the boundary conditions:

$$\begin{aligned} \Phi_I(\xi_0) &= \Phi_O(\xi_0) \\ \epsilon\;\frac{d\Phi_I(\xi)}{d\xi}\bigg|_{\xi=\xi_0} &= \epsilon_m\;\frac{d\Phi_O(\xi)}{d\xi}\bigg|_{\xi=\xi_0} \end{aligned} \tag{20}$$

and we find the coefficients $A_I$ and $B_O$ to be:

$$\begin{aligned} A_I &= \frac{\epsilon_m(h_1-h_2)}{\epsilon h_1 - \epsilon_m h_2} \\ B_O &= \frac{\epsilon_m - \epsilon}{\epsilon h_1 - \epsilon_m h_2} \end{aligned} \tag{21}$$

where the factors $h_1, h_2$ are given by:

$$\begin{aligned} h_1 &= \frac{\sqrt{1-\zeta^2}}{\zeta} \,-\, \tan^{-1}\left(\frac{\sqrt{1-\zeta^2}}{\zeta}\right) \\ h_1 - h_2 &= \frac{(1-\zeta^2)^{\frac{3}{2}}}{\zeta} \end{aligned} \tag{22}$$

and this gives us for the internal field $\mathbf{E}_I$:

$$\mathbf{E}_I = -\,A_I \boldsymbol{\nabla} G_0(\eta) F_0(\xi) \;=\; A_I\,\mathbf{E}_X. \tag{23}$$

The electric field outside $\mathbf{E}_O(\mathbf{r})$ has to be derived from:

$$\begin{aligned} \mathbf{E}_O(\mathbf{r}) &= \mathbf{E}_X \,-\, B_O \boldsymbol{\nabla} G_0(\eta) F_1(\xi) \\ &= \mathbf{E}_X \,+\, \mathbf{E}_E(\mathbf{r}). \end{aligned} \tag{24}$$

We refrain from the details and give only the final result in cylindrical coordinates:

$$\begin{aligned} \mathbf{E}_E(\mathbf{r}) &= E_\rho\,\hat{\boldsymbol{\rho}} \,+\, E_z\,\hat{\mathbf{z}} \\ \mathbf{r} &= \rho\,\hat{\boldsymbol{\rho}} \,+\, z\,\hat{\mathbf{z}} \;=\; \sqrt{x^2+y^2}\,\hat{\boldsymbol{\rho}} \,+\, z\,\hat{\mathbf{z}} \\ \hat{\boldsymbol{\rho}} &= \cos\phi\;\hat{\mathbf{x}} \,+\, \sin\phi\;\hat{\mathbf{y}} \end{aligned} \tag{25}$$

and the component fields $E_\rho, E_z$ are obtained as:

$$\begin{aligned} E_\rho &= -E_0 B_O \left[\frac{\tilde{z}\,\tilde{\rho}\,\sqrt{S}}{(S^2+\tilde{z}^2)\,(1+S)}\right] \\ E_z &= -E_0 B_O \left[\tan^{-1}\left(\frac{1}{\sqrt{S}}\right) \,-\, \frac{S\,\sqrt{S}}{S^2+\tilde{z}^2}\right] \end{aligned} \tag{26}$$

where the auxiliary variable $S$ is defined by:

$$\begin{aligned} S &= \sqrt{s^2+\tilde{z}^2} \,+\, s \\ s &= \frac{1}{2}\left[\tilde{\rho}^2 + \tilde{z}^2 - 1\right] \end{aligned} \tag{27}$$

whereas $\tilde{v} = v/f$ and $v = \rho, z$. Using these expressions for the outer field, back-transformation to cylindrical coordinates is established, but those coordinates are equivalent to Cartesian, because of the cylindrical symmetry of the problem. We treat in detail only the response in the $z$-direction. The response in the $x,y$-direction will be added later in a different way.

### 2.4 Embedded dielectric objects: excess polarization and field penetration

With the closed expressions for the electric fields obtained in the previous section we have all essential ingredients to investigate the consequences of embedding upon the optics of nano-objects. In top of that we have to account also for the bare or dressed character of the dynamical part $\Delta\alpha(\omega)$. Finally we will describe the optics of embedded nano-objects by means of a modified discrete dipole model. This requires a proper transformation of the results obtained until here and that transformation is the topic of this section. It starts by extracting physically meaningful quantities from the electric field expressions.

We start with the expression for the internal electric field (23) and use it to introduce the *field penetration* $f_E$, which determines the amount of the external field $E_0$,

which can enter the nano-object as its internal (average) field $E_I$:

$$f_E = A_I \;=\; \frac{\epsilon_m}{\epsilon_m + N_z(\epsilon - \epsilon_m)}$$

$$N_z = \frac{h_1}{h_1 - h_2}. \tag{28}$$

Although $f_E$ is just a redefinition, it highlights much better what happens physically. At the same time we introduce the *shape (or depolarization) factor* $N_z$, which depends only on the geometry of the nano-object. It is exclusively determined by the values of the eigenfunctions of the problem at the boundary $\xi_0$ and accounts for the shape dependence. We find for $N_z$:

$$N_z = \frac{1}{1-\zeta^2}\left(1 \,-\, \frac{\zeta\,\cos^{-1}\zeta}{\sqrt{1-\zeta^2}}\right) \tag{29}$$

where we have used the identity

$$\cos^{-1}\zeta = \tan^{-1}\left(\frac{\sqrt{1-\zeta^2}}{\zeta}\right). \tag{30}$$

This shape factor $N_z$ (29) is exactly the same as the shape factor obtained by Avelin [18]. It comes close to being a local continuum counterpart of the intracellular transfer tensor, but it is not its replacement. We define now two polarization densities:

$$\mathbf{P} = (\epsilon - 1)\epsilon_0\, f_E\, \mathbf{E}_X$$

$$\mathbf{P}_m = (\epsilon_m - 1)\epsilon_0\, f_E\, \mathbf{E}_X \tag{31}$$

where $\mathbf{P}$ is the full polarization density inside the nano-object and $\mathbf{P}_m$ the polarization density inside of it if the nano-object would have had the dielectric constant of the host, but with the internal field unaltered ($f_E$ remains the same function of $\epsilon_m$). We call this $\mathbf{P}_m$ the host part of the polarization density. When we use the generic relation (1) we can use these polarization densities to define corresponding dipole strength's and dressed polarizabilities:

$$\mathbf{p} = \alpha\,\mathbf{E}_X \;=\; f_E\,\alpha_B\,\mathbf{E}_X$$

$$\mathbf{p}_m = \alpha_m\,\mathbf{E}_X \;=\; f_E\,\alpha_{Bm}\,\mathbf{E}_X \tag{32}$$

and bare polarizabilities:

$$\alpha_B = (\epsilon - 1)\epsilon_0 V$$

$$\alpha_{Bm} = (\epsilon_m - 1)\epsilon_0 V. \tag{33}$$

When we replace in the expression for $\alpha_B$ the static $\epsilon$ by the dynamic $\epsilon(\omega)$, we obtain the full bare polarizability $\alpha_B(\omega)$ treated in Section 2.2. Why we introduce these polarizabilities becomes clear when we work out further the expression for the outer electric field. First we reformulate the coefficient $B_O$:

$$B_O = -\frac{F(\zeta)}{\epsilon_m}(\epsilon - \epsilon_m) f_E \epsilon_0 V \;=\; -\frac{F(\zeta)}{\epsilon_m}(\alpha - \alpha_m)$$

$$F(\zeta) = \frac{1}{\epsilon_0 V}\left(\frac{\zeta}{(1-\zeta^2)^{\frac{3}{2}}}\right) \tag{34}$$

where $V = \frac{4}{3}\pi a^2 c = \frac{4}{3}\pi\zeta a^3$ is the volume of the ellipsoid. This result allows us to write the expression for the outer field in a format which is required by the further discrete nonlocal treatment of this problem:

$$E_\rho = \frac{F(\zeta)}{\epsilon_m}\left[\frac{\tilde{z}\,\tilde{\rho}\,\sqrt{S}}{(S^2+\tilde{z}^2)\,(1+S)}\right]\Delta p$$

$$E_z = \frac{F(\zeta)}{\epsilon_m}\left[\tan^{-1}\left(\frac{1}{\sqrt{S}}\right) \,-\, \frac{S\,\sqrt{S}}{S^2+\tilde{z}^2}\right]\Delta p \tag{35}$$

where we used the following definitions:

$$\Delta p = p - p_m \;=\; \alpha_{DE}\,E_0 \;=\; \alpha_{BE}\,f_E\,E_0$$

$$\alpha_{BE} = \alpha_B - \alpha_{Bm} \;=\; f_C\,\epsilon_0 V$$

$$f_C = \epsilon - \epsilon_m \tag{36}$$

where $f_C$ is the *excess susceptibility*. This excess susceptibility $f_C$ controls the excess polarization density. The excess bare polarizability $\alpha_{BE}$ is the most important object parameter for embedded nano-objects. From the expression for the outer field we have to conclude that optically the nano-objects are dielectric protrusions, expressing themselves independently only by means of an excess polarization density and excess dipole strength $\Delta p$. For embedding the relevant dressed polarizability is not $\alpha$, but the dressed excess polarizability $\alpha_{DE}$:

$$\alpha_{DE} = \epsilon_0\epsilon_m V\left(\frac{\epsilon - \epsilon_m}{\epsilon_m + N_z(\epsilon - \epsilon_m)}\right). \tag{37}$$

For $\epsilon_m = 1$ this result produces also Avelin's vacuum polarizability [18]. For $\epsilon_m > 1$ the dressed excess polarizability above becomes really an embedded one. The other components of $\alpha_{DE}$ can be obtained by using the depolarization factors $N_x, N_y$:

$$N_x = N_y \;=\; \frac{1 - N_z(\zeta)}{2} \tag{38}$$

which is because the static transfer kernel has trace zero and the depolarization factor is just the volume integral of it. We classify this result as *local electromagnetic*. We use expression (36) for the bare excess polarizability $\alpha_{BE}$ and the nonlocal expression (5) for $\alpha_{DE}$:

$$\alpha_{DEu} = \left(\frac{\alpha_{BE}}{1 - t_{Eu}\,\alpha_{BE}}\right) \tag{39}$$

where $u = (x, y, z)$, to derive the embedded intracellular transfer tensor $\mathbf{t}_E$. The result is:

$$t_{Eu} = \frac{1}{\epsilon_m}\, t_u$$

$$t_u = -\frac{N_u}{\epsilon_0\, V} \tag{40}$$

where $\mathbf{t}$ is the corresponding tensor for the vacuum situation. For embedded nano-objects the intracellular transfer tensor $\mathbf{t}_E$ is screened by $\epsilon_m$, the dielectric constant of the embedding medium. For a nano-object in vacuum the intracellular transfer tensor $\mathbf{t}$ is, in contrast, *not* screened by the dielectric constant $\epsilon$ of the nano-object. Calculations start with the full bare polarizability $\alpha_B$ as will be dealt with in detail in Section 3. Next the bare excess polarizability $\alpha_{BE}$ takes over and enables the hybrid method to determine the excess dipole strength. From here on we will implicitly assume this excess character and omit mostly the excess qualifier. Similarly $\Delta\mathbf{p}$ will be replaced by $\mathbf{p}$ to improve reading.

We have collected all ingredients to specify the details of the hybrid model for the case of embedded nano-objects. The static interaction between more of these ellipsoids is governed by the *ellipsoidal transfer kernel* $\mathbf{t}^L(\mathbf{r})$. This transfer kernel is defined by:

$$\mathbf{E}_E(\mathbf{r}) = \frac{1}{\epsilon_m}\ \overleftrightarrow{\mathbf{t}}^{L}\ (\mathbf{r})\ \mathbf{p} \tag{41}$$

where the $\rho, z$ components were obtained already in equation (35) and we can write:

$$t^L_{\rho z}(\mathbf{r}) = F(\zeta)\left[\frac{\tilde{z}\,\tilde{\rho}\,\sqrt{S}}{(S^2+\tilde{z}^2)\,(1+S)}\right]$$

$$t^L_{zz}(\mathbf{r}) = F(\zeta)\left[\tan^{-1}\left(\frac{1}{\sqrt{S}}\right) - \frac{S\,\sqrt{S}}{S^2+\tilde{z}^2}\right]. \tag{42}$$

We show in the appendix, that this ellipsoidal transfer kernel converges rapidly to the classical dipolar transfer kernel $\mathbf{t}(\mathbf{r})$ which has been studied extensively by us and others [19,20]. For this paper the difference is small (at maximum 5% for the nearest neighbors) and we replace the ellipsoidal kernel by its dynamic dipolar equivalent for all intercellular interactions. Then we can set up the discrete part of the hybrid method. This requires no more but the systematic replacement above of the external field $\mathbf{E}_0$ by the local field $\mathbf{E}_L$, as follows:

$$\mathbf{E}_{Li} = \mathbf{E}_0 + \frac{1}{\epsilon_m}\sum_{j\neq i}\overleftrightarrow{\mathbf{t}}_{ij}\ \mathbf{p}_j \tag{43}$$

where $\mathbf{t}_{ij}$ is the vacuum intercellular transfer tensor, defined simply as:

$$\mathbf{t}_{ij} = \mathbf{t}(\mathbf{r}_i - \mathbf{r}_j) \tag{44}$$

with $\mathbf{r}_i, \mathbf{r}_j$ the center coordinates of the nano-objects. When $a \ll a_L \ll \lambda$, where $\lambda$ is the wavelength of the incoming light, the local field $\mathbf{E}_{Li}$ as expressed above is a good approximation. The transfer tensor is the discrete counterpart of the continuum transfer kernel. The induction for the dipole strength's $\mathbf{p}_i$ becomes now:

$$\mathbf{p}_i = \overleftrightarrow{\alpha}_{DE,i}\left[\mathbf{E}_0 + \frac{1}{\epsilon_m}\sum_{j\neq i}\overleftrightarrow{\mathbf{t}}_{ij}\ \mathbf{p}_j\right] \tag{45}$$

where $\alpha_{DE,i}$ is the dynamic dressed excess polarizability $\alpha_{DE,i}$. The system of equations to be solved becomes:

$$\overleftrightarrow{\alpha}^{-1}_{DE,i}\ \mathbf{p}_i - \frac{1}{\epsilon_m}\sum_{j\neq i}\overleftrightarrow{\mathbf{t}}_{ij}\ \mathbf{p}_j = \mathbf{E}_0. \tag{46}$$

This scheme of solution has not our preference. For all calculations we will use the dynamic bare excess polarizability $\alpha_{BE}$ (Eq. (36)), obtained as:

$$\alpha_{BE} = \alpha_B(\omega) - \alpha_{Bm}\ =\ (\epsilon(\omega) - \epsilon_m)\,\epsilon_0 V \tag{47}$$

where $\alpha_B(\omega)$ is either for added to bare from (10), or for added to dressed from (12). Then we only have to use (5) to change (46) into:

$$\overleftrightarrow{\alpha}^{-1}_{BE,i}\ \mathbf{p}_i - \frac{1}{\epsilon_m}\sum_{j}\overleftrightarrow{\mathbf{t}}_{ij}\ \mathbf{p}_j\ =\ \mathbf{E}_0$$

$$t_u = -\frac{N_u}{\epsilon_0\, V} + \frac{i\omega^3}{6\pi\epsilon_0 c^3} \tag{48}$$

where we have added the Lorentz radiation damping (the term with $\omega^3$ above) to the intracellular transfer tensor $t_u$ (second line above). This intracellular transfer tensor is added subsequently to the sum over transfer tensors (first line above). For a crystalline lattice plane (here a square lattice) the sums above can be calculated by a highly convergent series expansion (Vlieger approximation [21,22]). In this expansion the Lorentz radiation damping term will cancel with respect to a similar term in that expansion.

A last remark, but a very important one, concerns the correct transfer of the material properties of an isolated nano-object towards the embedded situation. This question can only be properly answered in the local continuum picture. In that picture the optical parameter governing the response of the object is the dielectric constant $\epsilon$. The rule now simply becomes that *embedding cannot change the dielectric constant of the nano-object*. Now we switch to the equivalent nonlocal discrete description of the nano-object. In that description the dressed polarizability depends upon the intracellular transfer tensor and the bare polarizability. The intracellular transfer tensor does not depend on $\epsilon$, as one can see from equation (40). Hence all dependency with respect to $\epsilon$ is in the bare excess polarizability $\alpha_{BE}$, equation (47). We see from that equation that the dielectric constant $\epsilon(\omega)$ is equivalent to the bare full polarizability $\alpha_B(\omega)$. If this bare full polarizability remains the same upon embedding (and it does) the nano-object keeps its correct material property $\epsilon(\omega)$. So the bare polarizability is the crucial carrier of information

going from vacuum to embedded, independently from how the dynamical part has been added. The type of addition has already been included in the dielectric constant $\epsilon(\omega)$ prior to embedding.

### 2.5 Effects of embedding

We have explained in detail the difference between bare and dressed polarizabilities at the beginning. The concepts of field penetration $f_E$ and excess susceptibility $f_C$ introduced in 2.4, determine completely the static behavior of the bare and dressed polarizabilities (addition of $\Delta\alpha$ can and will be ignored here), as is clear from the definitions:

$$\alpha_{DE} = f_E\, \alpha_{BE}$$
$$\alpha_{BE} = f_C\, \epsilon_0 V. \tag{49}$$

The static part of the polarizability is a dominant part of the polarizability also in the energy range we are interested in. We study it here separately. To understand its behavior it is hence enough to understand the two factors $f_E, f_C$, as given by equations (28, 36):

$$f_E = \frac{1}{1 + f_C\, N_u/\epsilon_m}$$
$$f_C = \epsilon - \epsilon_m. \tag{50}$$

Both factors have a clear physical meaning. We summarize that from the previous section. The field penetration $f_E$ gives the extent by which the external field can penetrate the nano-object. The excess susceptibility $f_C$ gives the amount by which the polarization of the nano-object increases when its dielectric constant changes from the host value to the nano-object value under application of the internal field inside the embedded object. In one glance the factors show the influence of embedding: embeddding affects $f_E$ by division by $\epsilon_m$ of the shape factor $N_u$ and affects $f_C$ by subtraction of $\epsilon_m$.

These effects can also be retraced in the behavior of the electric field. We show in Figure 3 the $z$-component of the electric field $E_z$ in the $xz$-plane (shown for the ellipsoid approximating the same quantum dot, as will be treated in Sect. 3). The electric field inside the quantum dot is prominent and indicates the amount of field penetration as given by $f_E$. The field contribution of the dielectric ellipsoid distorts strongly the field just outside the ellipsoid, but decays rapidly further away. The jump in electric field strength $\Delta E$ at the boundary of the ellipsoid is given by:

$$\frac{\Delta E}{E_0} = \frac{1}{\epsilon_m} f_E f_C \left[\frac{\sin^2\eta\,\sqrt{1-\zeta^2}}{\zeta^2 + \sin^2\eta\,(1-\zeta^2)}\right]. \tag{51}$$

The value $\eta = 0$ represents the $xy$-plane where there is no drop in electric field, as should be since $E_z$ is tangential there. For $\eta = \pi/2$ we are on the $z$-axis and then;

$$\Delta E = \frac{\sqrt{1-\zeta^2}}{\epsilon_0 \epsilon_m}(P - P_m). \tag{52}$$

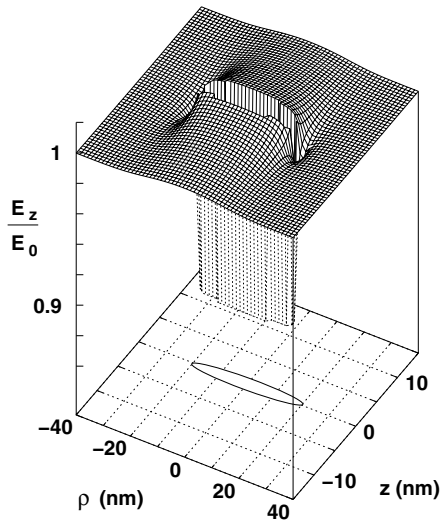


**Fig. 3.** Static electric field strength in units of $E_0$ in the $z$-direction for an embedded InAs/GaAs quantum dot in an external electric field $\mathbf{E}_0 = E_0\hat{\mathbf{z}}$.

There the electric field drop scales with the excess polarization density and not e.g. with the difference in polarization inside and just outside the ellipsoid. So $\Delta E$ is proportional to $f_C$. For the case shown in Figure 3 the value of $\Delta E = 0.137\, E_0$ and $f_E = 0.879$.

The following picture of embedding emerges. First the bare polarizability decreases from its vacuum value to the embedded excess value. Simultaneously the field penetration increases. The dressed polarizability governs the externally observable response for a single nano-object and depends on two antagonistic mechanisms accounted for by the factors $f_E, f_C$. We examine here in detail how the two factors behave statically.

For oblate ellipsoid-type of quantum dots the field penetration $f_E$ is shown in Figure 4. For that case the consequences of embedding upon this factor are very outspoken. When we use for the dielectric constants the InAs/GaAs values $\epsilon = 15.15$ and $\epsilon_m = 13.1$ [23], the field penetration $f_E$ increases by a factor of 11.9 for the $z$-component and by a factor of 1.8 for the $x$-component as compared to vacuum. So the increments caused by embedding are highly anisotropic. The reason of this anisotropic influence of embedding is in the large anisotropy of the depolarization factor $N_u$, or equivalently in $t_u$. For values of $\epsilon$ below $\epsilon_m$ ($\epsilon < 13.1$) this results even in a reversal of the anisotropy and a field penetration larger than 1. For InAs there is not yet reversal, but the anisotropic change of the dressed polarizability results into an almost disappearance of the externally observable anisotropy. The field penetration $f_E$ is for the InAs case 0.878 for the $z$-direction and 0.991 for the $x$-direction. The consequences are twofold. First the difference between internal and external field has become almost negligible. Next the anisotropy has almost vanished. Both phenomena have the same origin. In the expression for the field penetration $f_E$, equation (50), the influence of the shape $N_u$ has been severely weakened by the $\epsilon_m$.

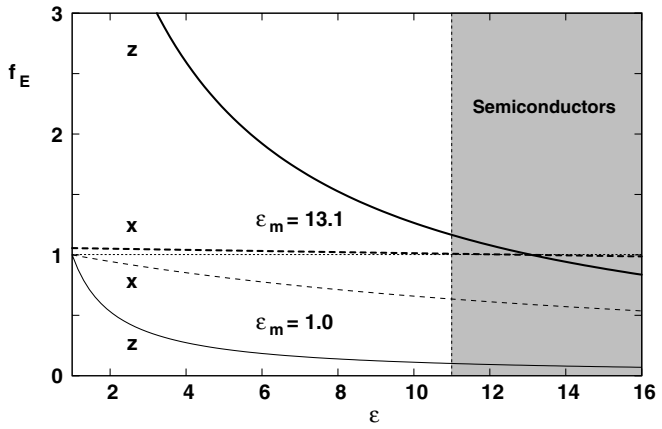


**Fig. 4.** Field penetration $f_E$ for an oblate ellipsoid as a function of its dielectric constant $\epsilon$. Shaded: semiconductor regime. The two upper curves are for $\epsilon_m = 13.1$, the embedded case, and the two lower curves are for $\epsilon_m = 1$, the vacuum case. $x$ (dashed), $z$ (solid) Cartesian directions.

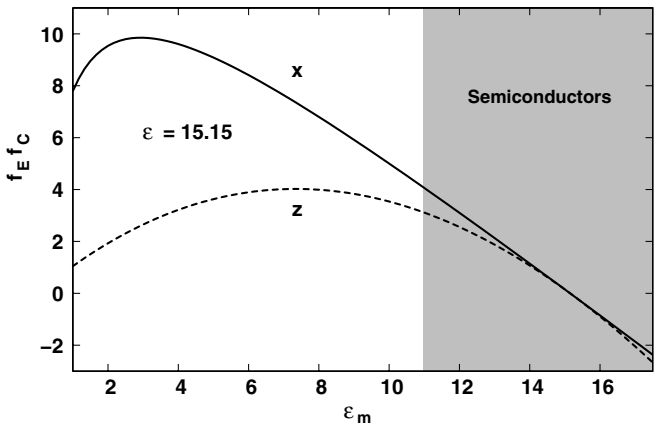


**Fig. 5.** Combined field penetration and excess factors $f_E f_C$ for an oblate ellipsoid with $\epsilon = 15.15$ as a function of the host dielectric constant $\epsilon_m$. Shaded: semiconductor regime. $x$ (dashed), $z$ (solid) Cartesian directions.

The excess susceptibility $f_C$ as such has a trivial behavior. This factor is important because it is the antagonist of the field penetration $f_E$. Because of this antagonistic behavior somewhere a maximum will be encountered. We cast the influence of both factors into a single expression for the dressed, hence externally observable, polarizability $\alpha_{DE}$:

$$\alpha_{DE} = f_E f_C \, \epsilon_0 V. \tag{53}$$

The behavior of the combined factors $f_E f_C$ is shown in Figure 5 as a function of the dielectric constant $\epsilon_m$ of the hostmaterial. Both for the $x$-direction and for the $z$-direction the maximum is found inbetween the vacuum value of $\epsilon_m = 1$ and the value of $\epsilon_m = 13.1$ for the current host (GaAs). Applying basic differentiation rules to $f_E f_C$, yields upon requiring that the numerator has to be zero, that the maximum is at $\epsilon_{m0}$, given by:

$$\epsilon_{m0} = \frac{\sqrt{N_u}}{1 + \sqrt{N_u}} \, \epsilon. \tag{54}$$

These maxima, obtained for $\epsilon_m \approx 3.02$ for the $x$-direction and $\epsilon_m \approx 7.32$ for the $z$-direction, are well above the value of the vacuum polarizability. This is remarkable, because these results are directly proportional to the dressed *excess* polarizability, although one has to bear in mind that for $\epsilon_m \to 1$ that polarizability becomes the vacuum polarizability itself.

### 2.6 Electromagnetic response

The calculation of the optical response of an embedded square lattice (monolayer) of quantum dots can be performed using the same (Vlieger) expressions [21,22] for the reflected electric fields from a square lattice with lattice constant $a_L$, as used before in [6]:

$$r_{ss} = \frac{f_k}{A_y \cos\theta_i - f_k}$$

$$r_{pp} = \frac{f_k \cos\theta_i}{A_x - f_k \cos\theta_i} - \frac{f_k \, \sin^2\theta_i}{A_z \cos\theta_i - f_k \, \sin^2\theta_i}. \tag{55}$$

The following abbreviations are used to make the expressions more concise, but they contain also all elements which change, when the nano-object gets embedded:

$$A_u = \alpha_0 \, \alpha_{BEu}(\omega)^{-1} - \frac{1}{\epsilon_m} \, (\mathsf{f}_u + \mathsf{t}_u)$$

$$f_k = 2\pi i a_L k_m \tag{56}$$

where $\alpha_0 = 4\pi\epsilon_0 a_L^3$. We use here the solution scheme given in equation (48), based upon the bare excess polarizability (47) and combination of the intracellular transfer tensor $\mathbf{t}$ with the planar transfer tensor $\mathbf{f}$ [19]. Both tensors are made dimensionless through $\mathsf{f} = \alpha_0 f$ and $\mathsf{t} = \alpha_0 t$. All transfer tensors are screened, as described before. The wavenumber $k_m$ changes also upon embedding, as will be treated now.

Since the Vlieger equations are dynamical they contain the wave number $k$, which is directly affected by the dielectric constant $\epsilon_m$ of the embedding medium, because it follows from the dispersion equation for the embedding medium:

$$\nabla^2 \mathbf{E} - \epsilon_0 \mu_0 \epsilon_m \frac{\partial^2}{\partial t^2} \mathbf{E} = 0.$$

We refer to the wave number inside the medium as $k_m$ and to the vacuum wave number as $k_0 = \omega/c$. The result becomes:

$$k_m = \sqrt{\epsilon_m} \, \frac{\omega}{c} \; = \; \sqrt{\epsilon_m} \, k_0.$$

The embedded wave number $k_m$ turns out to be almost 4 times (3.62) as large as the vacuum wave number $k_0$ for GaAs and affects the reflection coefficients by the same amount, as can be seen from equation (55).

**Table 1.** Basic input parameters for lattices of InAs/GaAs quantum dots. For meaning of symbols: see text

| | |
|---|---|
| $a_L$ | 80.0 nm |
| $a$ | 18.45 nm |
| $c$ | 1.49 nm |
| $\lvert\langle F_{h0}\rvert F_{e0}\rangle_V\rvert$ | 0.9 |
| $\lvert\langle F_{h,-1}\rvert F_{e,-1}\rangle_V\rvert$ | 0.9 |
| $\lvert\langle F_{h,-2}\rvert F_{e,-2}\rangle_V\rvert$ | 0.9 |
| $r_{eh}$ | 0.60 nm |
| $\epsilon$ | 15.15 |
| $\epsilon_m$ | 13.1 |
| $\hbar\gamma$ | 5.0 meV |

## 3 Numerical results

We show the results of the influence of embedding upon the optical response of an embedded square lattice of nano-objects for the case of quantum dots. We use the same geometry for the lattice of InAs-quantum dots as studied in [6], but now embedded in a GaAs-host. The dots are statically modelled by oblate dielectric ellipsoids with $a, c$ as the long, resp. short axis. The relevant data are given in Table 1. For further details we refer to [6].

In this comparative study where we examine the consequences of the addition of the dynamical polarizability to the bare or to the dressed polarizability, we have to start from the bare full polarizability $\alpha_B$ under static conditions. This polarizability is the same, as mentioned, as the bare excess polarizability $\alpha_{BE}$ for vacuum. Without addition of the quantum mechanical $\Delta\alpha(\omega)$ this bare polarizability would be isotropic and not influenced by the added to bare or added to dressed choice. We refer to the static value of the added to bare polarizability by $\alpha_{BB}$ and to that of the added to dressed polarizability by $\alpha_{DB}$. We get for $\alpha_{BB}$, using equation (10):

$$\alpha_{BBx} = 4.69401 \times 10^{-3}\ \alpha_0$$
$$\alpha_{BBz} = 4.68837 \times 10^{-3}\ \alpha_0 \qquad (57)$$

where the standard polarizability $\alpha_0$ has the value $5.69677 \times 10^{-32}$ Fm$^2$ for the lattice chosen in [6]. The faint anisotropy is caused by the static tail of the transitions incorporated in the $\Delta\alpha(\omega)$. For the $\alpha_{DB}$ we get, using equations (12) and (40):

$$\alpha_{DBx} = 4.706978 \times 10^{-3}\ \alpha_0$$
$$\alpha_{DBz} = 4.68837 \times 10^{-3}\ \alpha_0. \qquad (58)$$

The $z$-component is not different from the added to bare result, but that should be because the $z$-component does not contain $\Delta\alpha(\omega)$. There is however already a slight difference between the $x$-components of the two options. This difference, as we will show, will only increase a lot dynamically, if the quantum mechanical transitions will be at resonance. These bare polarizabilities are for quantum dots in vacuum. To turn these bare vacuum polarizabilities into bare embedded ones, requires subtraction of $\alpha_{Bm}$, which acts like a threshold polarizability. The value of $\alpha_{Bm}$ is for this case, using (33):

$$\alpha_{Bm} = 4.0091 \times 10^{-3}\ \alpha_0. \qquad (59)$$

As a result the bare embedded polarizability attains the value:

$$\alpha_{BEz} = 6.79234 \times 10^{-4}\ \alpha_0 \qquad (60)$$

where we give only the $z$-component since this does not depend on the type of addition and the $x$-components are very close to this value for the static case. This decrement of the bare polarizability upon embedding is also directly understood using the concept of the excess susceptibility $f_C$.

**Table 2.** Dressed static polarizability $\alpha_D$ for $x, z$-orientation for vacuum and embedded (excess values) situation.

| | Vacuum | Embedded |
|---|---|---|
| $\alpha_{Dx}$ | $2.58309 \times 10^{-3}\ \alpha_0$ | $6.91440 \times 10^{-4}\ \alpha_0$ |
| $\alpha_{Dz}$ | $3.46774 \times 10^{-4}\ \alpha_0$ | $5.96624 \times 10^{-4}\ \alpha_0$ |

Although internally for all calculations the bare polarizability is the main carrier of information, the externally observable consequences are only displayed by the dressed (excess) polarizability. We have collected these dressed polarizabilities in Table 2 both for the vacuum and embedded situation. These results are based upon the single $\alpha_{BEz}$ given in (60), since under static conditions the type of addition has hardly any influence. We observe in this table the trends discussed already in the previous section. The $x$-component drops by almost a factor of 4 upon embedding. The reason is that the depolarization factor $N_x$ is small (0.062), so $f_E$ increases only a little (1.8 times), whereas $f_C$ decreases by a full factor of 6.9. The $z$-component behaves very different. It increases upon embedding and becomes even stronger than the vacuum result. This behavior is exactly as shown in and discussed for Figure 5. Statically the consequences of embedding hence are strong, although certainly at first glance counter-intuitive. How we add the quantum mechanical $\Delta\alpha(0)$ however has only very weak influence.

The frequency dependent behavior of the $x$-component of the bare excess polarizability $\alpha_{BE}$ is shown in Figure 6 for its real part and in Figure 7 for its imaginary part. For all further calculations in this paper we will use for the damping term the value $\hbar\gamma = 5$ meV [6]. Each panel of each figure shows a direct comparison between the added to bare polarizability and the added to dressed polarizability. The added to bare polarizability has been obtained using equation (10) and the added to dressed polarizability using equation (12) and subsequently for both equation (36). A first inspection reveals immediately that adding to the dressed polarizability increases strongly (roughly by a factor of 4) any variation in the polarizability for this quantum dot-host combination. Here it pays off to use the field penetration concept. The added to bare polarizability $\alpha_{BB}(\omega)$ is simply:

$$\alpha_{BB}(\omega) = \alpha_B + \Delta\alpha(\omega) \qquad (61)$$

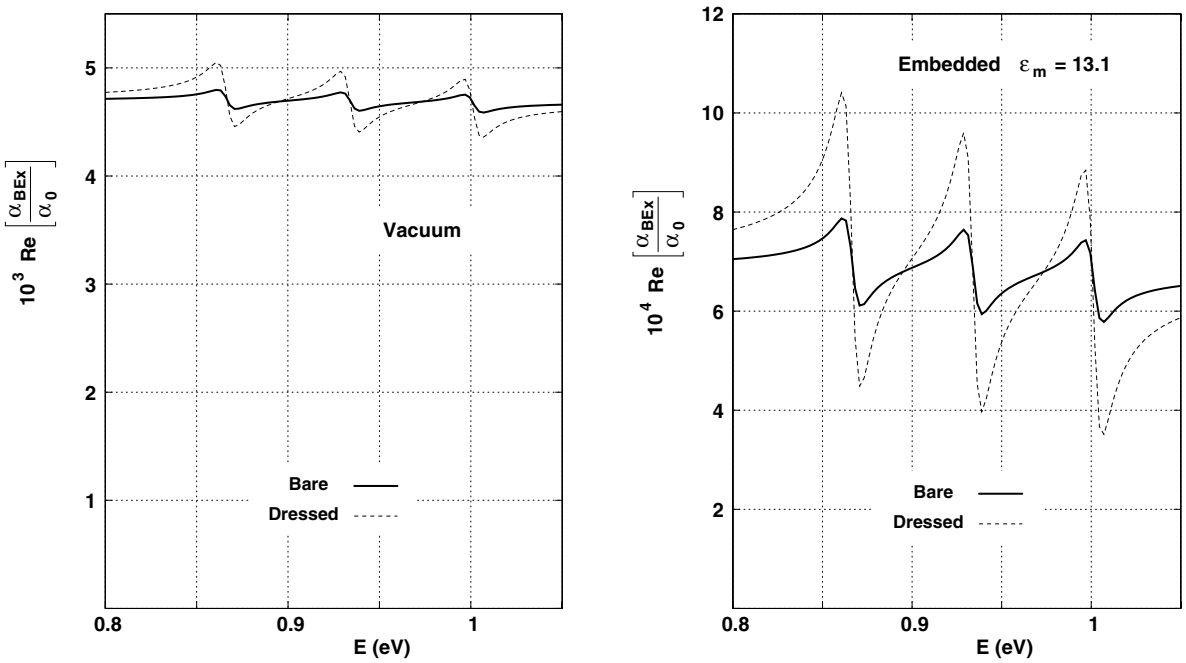


**Fig. 6.** Added to dressed versus to bare, real part of bare excess polarizability $\alpha_{BEx}/\alpha_0$. (a): Vacuum case; (b) embedded case with $\epsilon_m = 13.1$.

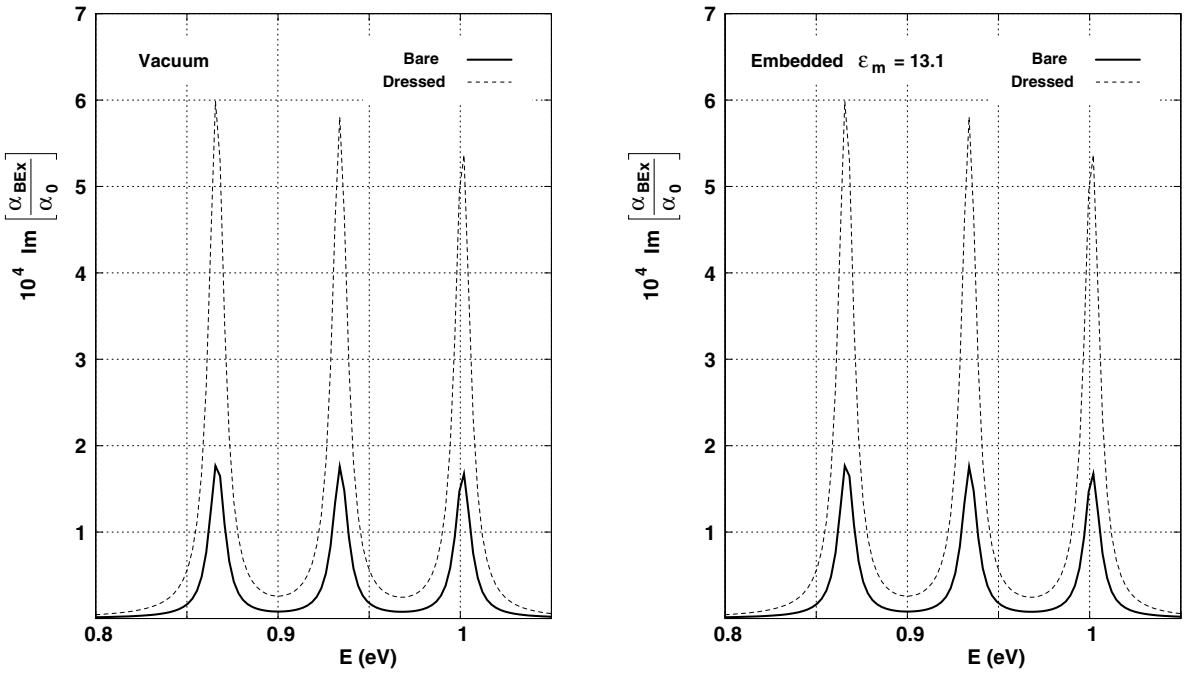


**Fig. 7.** Dressed versus bare, imaginary part of bare excess polarizability $\alpha_{BEx}/\alpha_0$. (a): Vacuum case; (b) embedded case with $\epsilon_m = 13.1$.

but for the added to dressed polarizability $\alpha_{DB}(\omega)$ we need two steps:

$$\alpha_D(\omega) = f_E\alpha_B + \Delta\alpha(\omega) = f_E(\omega)\alpha_{DB}(\omega)$$
$$\alpha_{DB}(\omega) = \frac{f_E}{f_E(\omega)}\left[\alpha_B + \frac{\Delta\alpha(\omega)}{f_E}\right] \quad (62)$$

where $f_E$ is the static and $f_E(\omega)$ the dynamic field penetration. Now the addition of $\Delta\alpha(\omega)$ is divided by $f_E = 0.532$ or multiplied by 1.88. In general $f_E(\omega) < f_E$, so the front factor is larger than 1. Both observations explain what is shown in the figures. The excess mechanism explains the change of the added to bare polarizability upon embedding. The factor $(\epsilon - 1)/(\epsilon - \epsilon_m)$ between vacuum and embedded has the value 6.9 and can be recognized

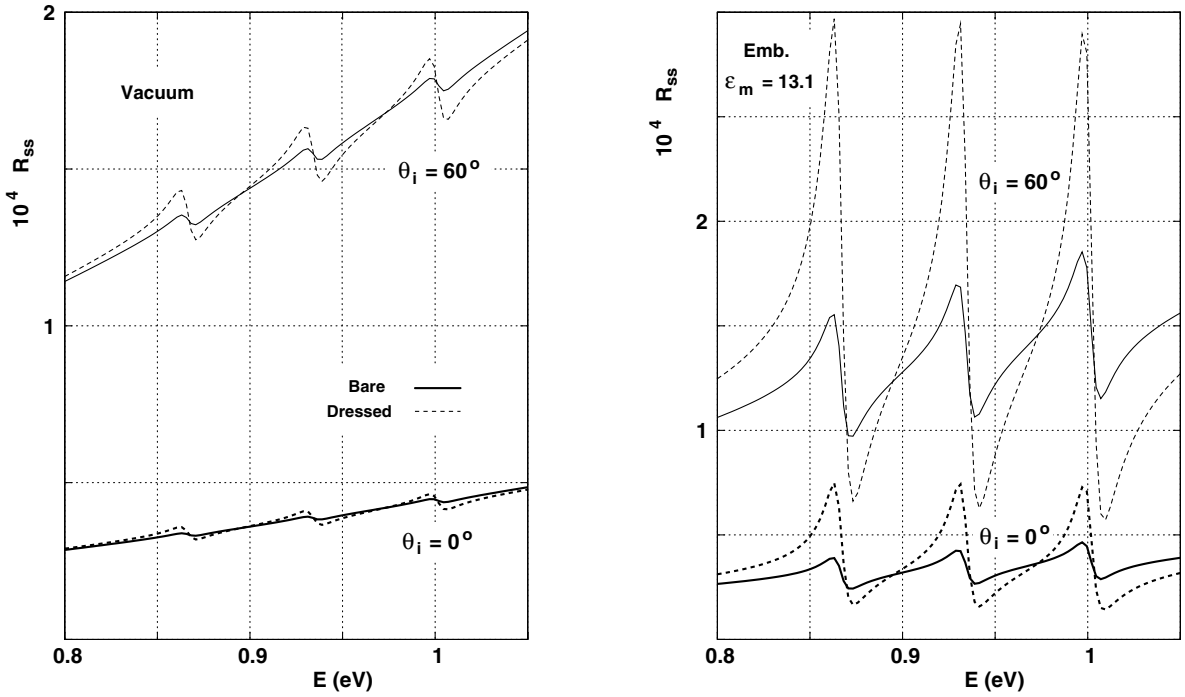


**Fig. 8.** Reflectance $R_{ss}$ for angles of incidence $\theta_i = 0°, 60°$. (a): Vacuum case; (b) embedded case with $\epsilon_m = 13.1$.

for the low energy results near $E = 0.8$ eV. The largest variations in the value of the real part are displayed by the added to dressed polarizability for the embedded case. Notice also the large offset for the vacuum real part results. The consequence of this offset is that the relative variations in the embedded results will be larger by a factor of 4 to 5 than for the vacuum results. A clear difference in behavior can be noticed between the real and imaginary part. The real part reacts upon any change, either from vacuum to embedded or from the one type of addition to the other. The imaginary part reacts only upon a change of the type of addition and is indifferent upon changes in the host dielectric constant $\epsilon_m$. This is obvious for the added to bare polarizability, but it turns out to hold for the added to dressed result as well. The value of the imaginary part increases by almost a factor of 4 going from bare to dressed addition and this is much. All imaginary parts are positive and this is as physics demands.

The first (internally) observable optical response term is the reflectance. For a single monolayer these reflectance's are weak. Embedding however does not deteriorate that situation much. For the angles of incidence of $\theta_i = 0°, 60°$ the reflectance's for the two polarization directions $s$ and $p$ are shown in Figures 8, 9. In these figures thick lines belong to $\theta_i = 0°$ and thin lines to $\theta_i = 60°$. The angle of $\theta_i = 60°$ is close to the Brewster angle, where $s$-type of reflectance is always (much) stronger than for $p$-type. Figure 8 shows the $ss$-reflectance in the area of interest ($0.8$ eV $< E = \hbar\omega < 1.05$ eV). To understand the results the following approximation for the Vlieger expression, equation (55), is useful:

$$r_{ss} \approx \frac{f_k\ \alpha_{By}}{\alpha_0\ \cos\theta_i} \tag{63}$$

where the factor $\sqrt{\epsilon_m}$ in $f_k$ changes upon embedding and causes the reflectivity to increase by 3.62 (13.1 for the reflectance), independent from the type of addition. All other changes in $r_{ss}$ are due to the bare polarizability $\alpha_{By}$. For both types of addition the real part of the polarizability decreases upon embedding by roughly a factor of 5, causing the reflectivity to increase by about 2. This tendency of the real part to decrease the reflectivity is disturbed by the imaginary part which is not influenced by embedding. The final result is that the overall reflectivity remains about the same for the added to bare and added to dressed cases. Only at he high energy side there is some decrement, but the relative variations in the reflectance are strongly enhanced for all cases upon embedding. This enhancement is about a factor of 4 for $\theta_i = 0°$ and for upto a factor of 10 for $\theta_i = 60°$.

For the $p$-component the situation is different. The angle $\theta_i$ is close to Brewster's angle and therefore the two terms composing $r_{pp}$ in equation (55) are of comparable strength. This explains the reversal of the $R_{pp}$ curves: the Brewster angle moves then from the one side of $\theta_i$ to the other. Because of the cancellation of the two terms in $r_{pp}$ a simple explanation as for $r_{ss}$ is not possible. Definitely the overall value of $R_{pp}$ is decreased (by one order of magnitude) with respect to $R_{ss}$ as should be the case. The influence of the dynamical part however seems to be unharmed. The fact that the low energy embedded values for the added to dressed are lower than for the the added to bare reflectance can only be understood by assuming that the first result is closer to the Brewster angle than the second. For both types of addition relative variations increase strongly upon embedding. The highest increment is for added to dressed, but that is clear in view of equation (62).

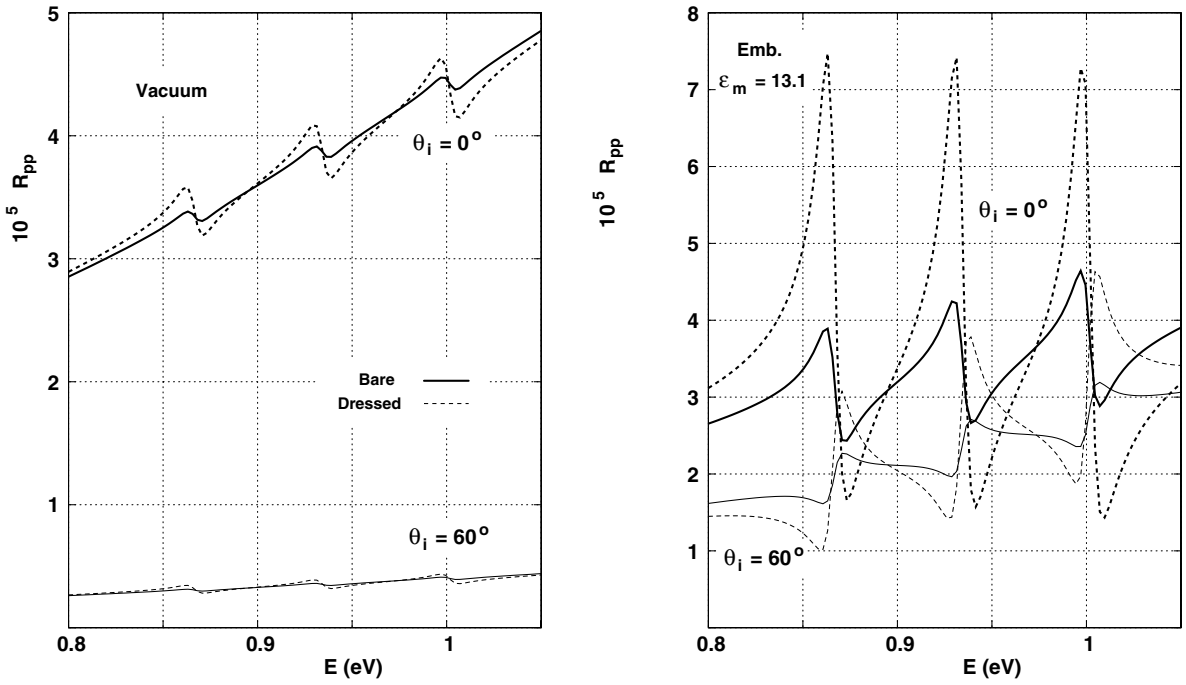


**Fig. 9.** Reflectance $R_{pp}$ for angles of incidence $\theta_i = 0°, 60°$. (a): Vacuum case; (b) embedded case with $\epsilon_m = 13.1$.

For both the $R_{ss}$ and $R_{pp}$ reflectances, as shown in Figures 8, 9, it is clear that the vacuum and embedded results are very different as concerns the character of the dynamic polarizability. For nano-objects in vacuum there is little influence whether we use the dynamical part $\Delta\alpha(\omega)$ as dressed or as bare. Upon embedding however the differences increase considerably, upto a factor of 5. This means that is should be relatively easy to use experimental data to decide which of the two options, bare or dressed, is the better one.

To complete the picture of the influence of embedding upon the externally observable response, as discussed for Figure 5 in Section 2.5, we show the reflectances $R_{pp}$, $R_{ss}$ in Figure 10 as a function of $\epsilon_m$. This figure allows for a conclusion similar to the one made there: also the embedded (pp)-reflectance can be larger than the vacuum reflectance. We also see clearly that for $\epsilon_m \approx 4.5$ the Brewster angle should be close to 60°, because we see the corresponding minimum. A possible replacement of the host material by GaP, having $\epsilon_m = 11.11$ [23] would result in an even stronger internal reflectance, as Figure 5 shows. Figure 5 also reveals that the closer $\epsilon$ gets to the host dielectric constant $\epsilon_m$, the better it becomes to discriminate between the types of addition, but it is also quite likely that then the model as such will loose validity.

In Figures 11, 12 we show the absorbances for the lattice of quantum dots. In Figure 11 are the results for $s$- and in Figure 12 for $p$-polarization. The $p$-type absorbances are by one order of magnitude below the $s$-type absorbances. For isotropic polarizabilities the absorbance would not have depended on polarization. Since the imaginary part of the polarizability of the quantum dots however is highly anisotropic in the region of interest, the absorbance becomes polarization dependent, as elucidated before in [7]. The absorbances in the figures have been calculated using Poynting's theorem:

$$A = 1 - (R + T) \tag{64}$$

where $A$ is the optical absorbance and $R, T$ the reflectance, transmittance resp. [6]. A simple, direct explanation of the calculated results is not possible here, so we comment only the general observed trend. The added to dressed results are always systematically above the added to bare results. This is in agreement with the behavior of the imaginary part of $\alpha_B$ as shown in Figure 7. The embedded absorbances are all above the vacuum absorbances by one order of magnitude. Partly this can be understood from the increased field penetration. For near static conditions $f_E$ increases by roughly a factor of 2 for this case and this factor should influence the absorbance as its square, amounting in a factor of 4. This analysis however is based upon the local absorption inside the nano-objects. This absorption is proportional, but not identical to the optical absorbance. There is no straightforward interpretation of the $p$-type of absorbance, beyond what we have written already.

The ellipsometric angles $\Psi$ and $\Delta$ are the experimental values which can be measured with the highest accuracy. They obey the definitions:

$$\frac{r_{pp}}{r_{ss}} = \tan\Psi e^{i\Delta} \tag{65}$$

and are relative quantities not dependent upon the absolute intensities of the reflected light. To this has to be

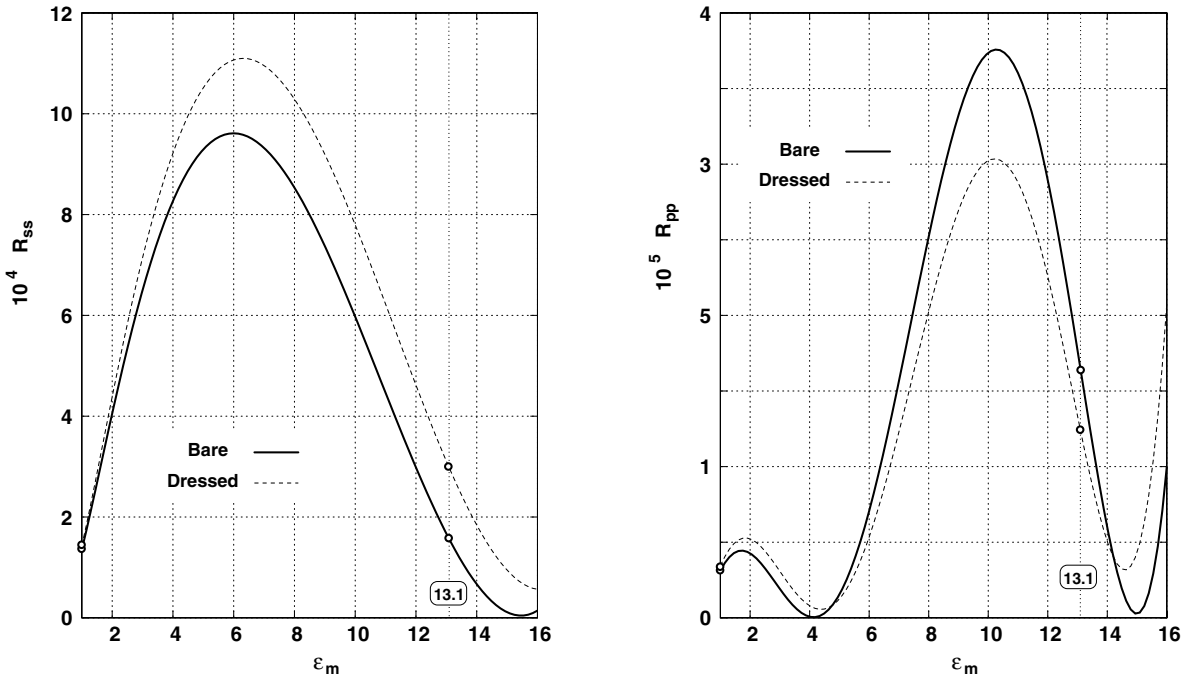


**Fig. 10.** Reflectances $R_{pp}$, $R_{ss}$ for varying $\epsilon_m$. The angle of incidence is $\theta_i = 60°$, $E = 0.863$ eV. Dielectric constant of the quantum dot is $\epsilon = 15.15$. Results for added to bare (solid) and added to dressed (dashed).

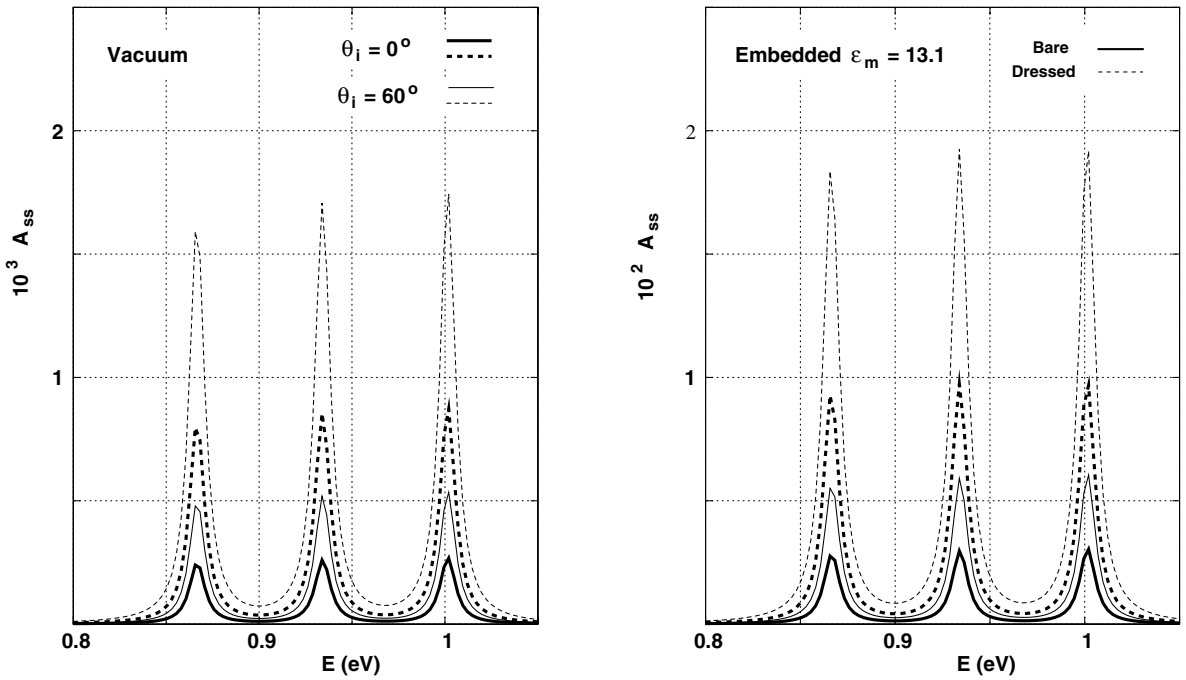


**Fig. 11.** Absorbance $A_{ss}$ for angles of incidence $\theta_i = 0°, 60°$. (a): Vacuum (no embedding); (b) embedding with $\epsilon_m = 13.1$.

added that the internal reflection (and transmission) coefficients of embedded nano-objects are in principle measurable, different from the free floating dots treated by us before [6]. Again we see that the added to dressed results are considerably stronger than the added to bare results. Both $\Psi$ and $\Delta$ however increase strongly upon embedding. In general $\Psi$ resembles in character the real part of the absorbance, as shown in Figure 6, and $\Delta$ resembles the imaginary part, as shown in Figure 7. Both responses "turn upside down", because the Brewster angle moves upon embedding. The relative variations in both $\Psi, \Delta$ improve by at least one order of magnitude upon embedding. This holds particularly for $\Delta$ where the enhancement goes up to two orders of magnitude already for the added to

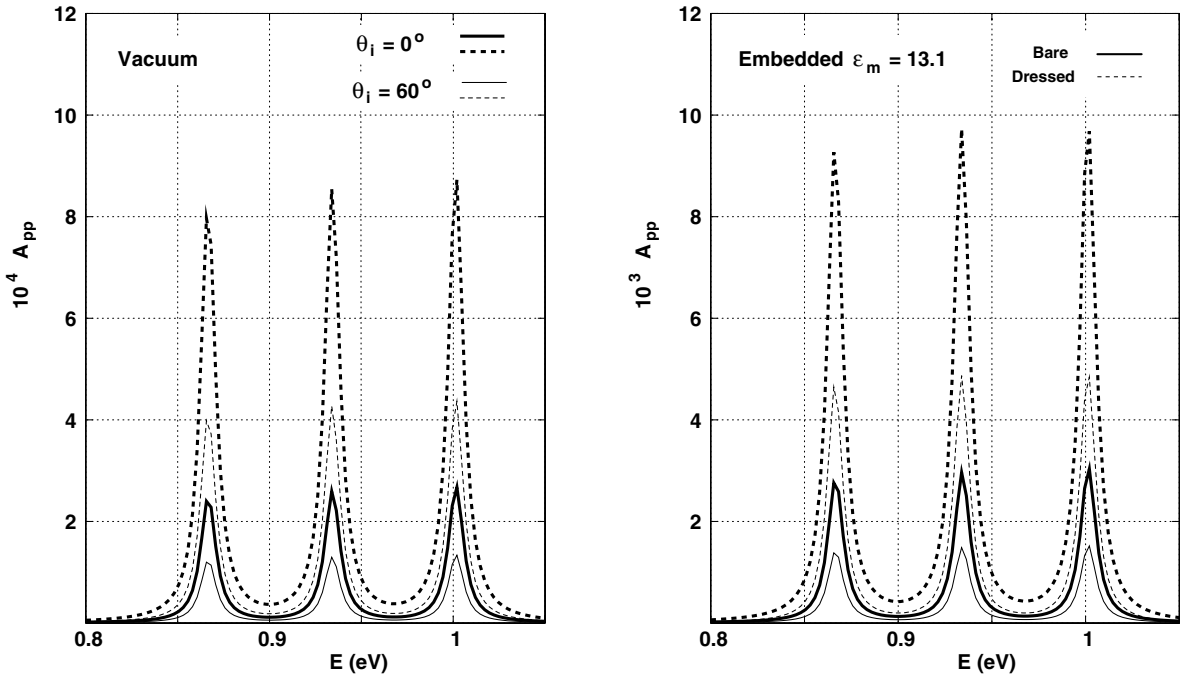


**Fig. 12.** Absorbance $A_{pp}$ for angles of incidence $\theta_i = 0°, 60°$. (a): Vacuum (no embedding); (b) embedding with $\epsilon_m = 13.1$.

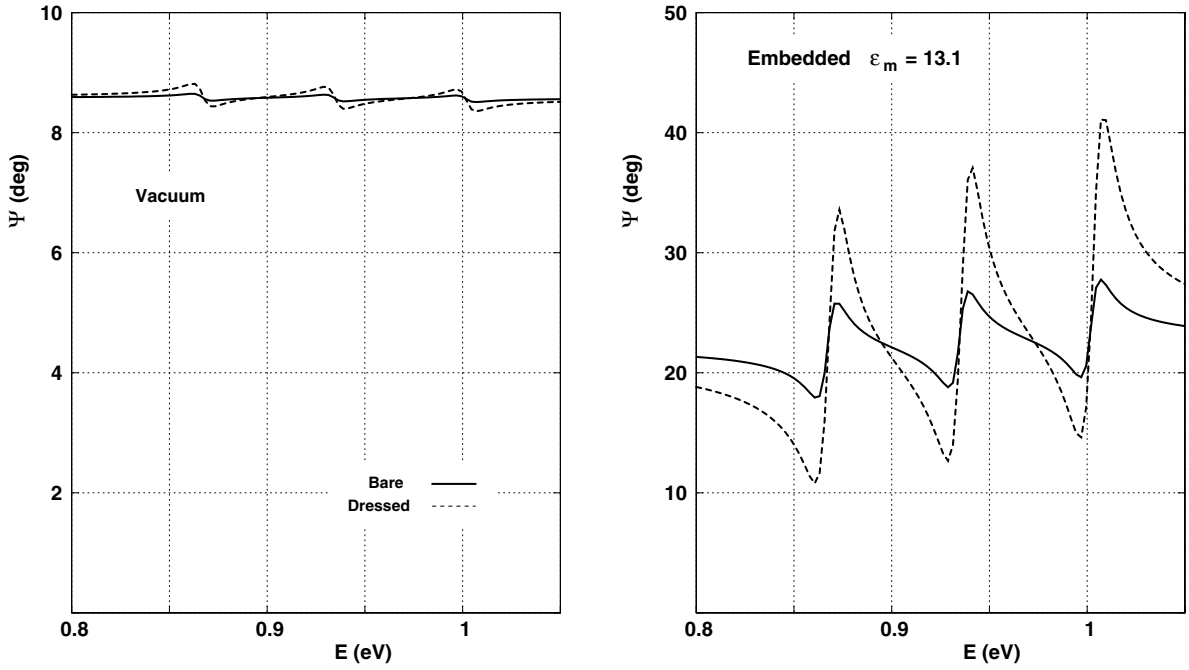


**Fig. 13.** Ellipsometric angle $\Psi$ for angle of incidence $\theta_i = 60°$. (a): Vacuum (no embedding); (b) embedding with $\epsilon_m = 13.1$.

bare results. The strongest variations are displayed by the added to dressed results, so the maximum theoretical variations are found for embedded added to dressed results. All ellipsometric results are comfortably within the range of a modern ellipsometer, provided the 4 to 5 orders of loss in intensity upon reflection can be coped with. Some indication that this is realistic can be derived from [24], where a commercial ellipsometer was used to measure a 100 nm layer of about 15 nm CdTe nanoparticles without noticeable noise.

## 4 Summary and conclusions

For a system of nano-objects (here quantum dots) we have derived a hybrid discrete-continuum model to investigate the changes in optical response of a square lattice of these

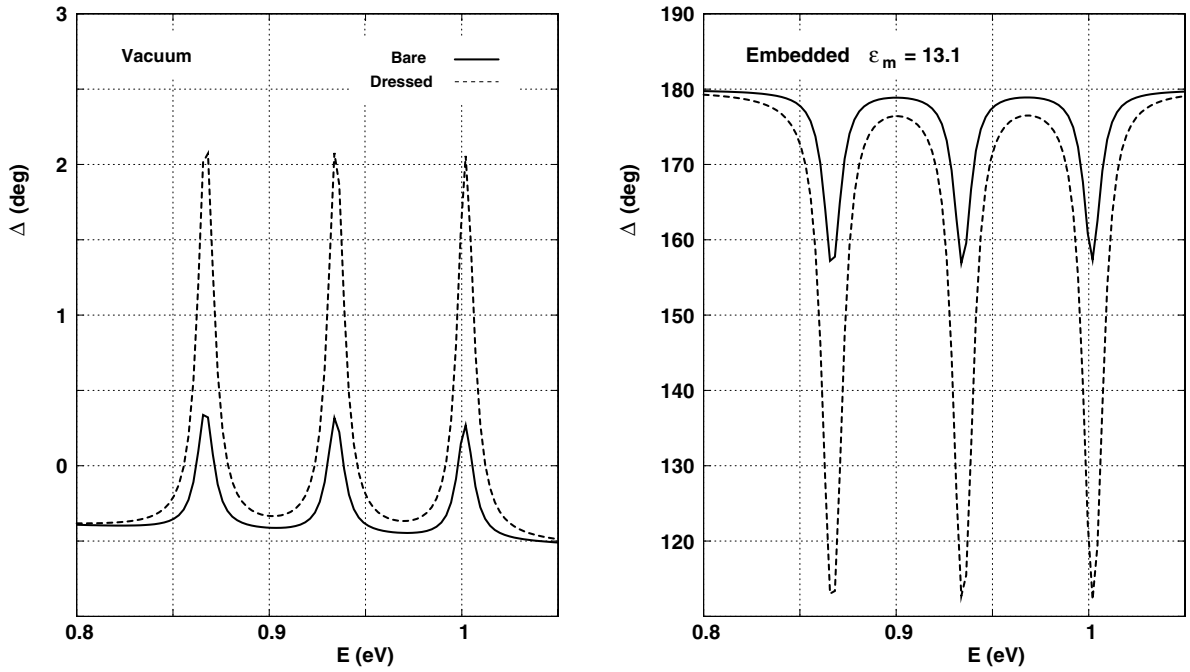


**Fig. 14.** Ellipsometric angle $\Delta$ for angle of incidence $\theta_i = 60°$. (a): Vacuum (no embedding); (b) embedding with $\epsilon_m = 13.1$.

dots upon embedding. The behavior of this model can be understood in terms of field penetration and excess susceptibility. These mechanisms determine what happens when the dots get embedded in a dielectric host material. The role of the excess susceptibility is clear in the sense that it is directly responsible for the representation of the optical response of the embedded lattice by excess discrete dipoles and excess bare polarizabilities. All electromagnetic interactions in a nonlocal picture however turn out to be screened by the host dielectric constant. This may seem obvious, but the internal electromagnetic interactions inside a free quantum dot are, in contrast, not screened. It is possible and also recommendable to use bare polarizabilities as the main carrier of information for the optical response. That results in a shorter and more transparent theoretical description, although it is definitely possible to use dressed polarizabilities also. The appealing idea to use a derivation where any dressed polarizability (the measured one!) is absent is frustrated by a fundamental problem caused by the dynamical part of the polarizability. Although from the theoretical point of view there is a preference to regard the quantum mechanical expression for that part as a bare polarizability, that identification is not really certain. It could also be dressed in nature. It is not the purpose of this paper to resolve this long-standing issue. Rather we have done all derivation and calculations for both options. The two options share the same general trends. Both give stronger to much stronger response for the embedded than for the vacuum case and the relative variation in the optical response is even more enhanced. The ellipsometric response given by the angles $\Psi, \Delta$ is with several tens of degree very strong. The difference between the added to bare and added to dressed options is in the systematically stronger results for the latter. This enhancement becomes even puzzling since the real part of the added to dressed polarizability can become negative. This does not reject the added to dressed option on physical grounds however, although it is definitely not normal dielectric behavior. The wiser decision to accept or reject any of the two options seems to be to do the measurements and to decide according to what those provide.

## Appendix A: Ellipsoidal transfer tensor: remote behavior

In this paper we need that the ellipsoidal transfer kernel/-tensor approaches closely the dipolar transfer kernel/tensor at large distances from the center of the ellipsoid. From general considerations of electrodynamics it is obvious that this has to be so, but here we show it explicitly for this particular case. We will use the original solutions for $E_\rho$ and $E_z$:

$$t^L_{\rho z}(\mathbf{r}) = F(\zeta)\left[\frac{\sin\eta\,\cos\eta}{(\sinh^2\xi+\sin^2\eta)\,\cosh\xi}\right]$$

$$t^L_{zz}(\mathbf{r}) = F(\zeta)\left[\tan^{-1}\left(\frac{1}{\sinh\xi}\right)-\frac{\sinh\xi}{\sinh^2\xi+\sin^2\eta}\right]. \quad (66)$$

The distance $r$ is expressed in ellipsoidal coordinates as:

$$r^2 = f^2[\cosh^2\xi-\sin^2\eta] \;=\; f^2[\sinh^2\xi+\cos^2\eta] \quad (67)$$

which for large $\xi$, corresponding to large $r$, can be approximated by:

$$f\cosh\xi \approx f\sinh\xi \approx r \quad (68)$$

and further it is useful to know that:

$$f^3 F(\zeta) = \frac{1}{\epsilon_m} \frac{3}{4\pi\epsilon_0} \tag{69}$$

we rewrite the field expression in the long range limit and expand it to the order of $r^{-2}$. For the $zz$-component we have:

$$\frac{t^L_{zz}(\mathbf{r})}{F(\zeta)} \approx -\frac{1}{3\sinh^3\xi} + \frac{\sin^2\eta}{\sinh^3\xi} \tag{70}$$

where we have used that $\tan^{-1}(x) \approx x - \frac{1}{3}x^3$ and that $1/(1+x) \approx 1 - x$,

$$\begin{aligned} t^L_{zz}(\mathbf{r}) &\approx \frac{f^3 F(\zeta)}{3r^3}\left[3\sin^2\eta - 1\right] \\ &= \frac{1}{\epsilon_m}\frac{1}{4\pi\epsilon_0 r^3}\left[3\sin^2\eta - 1\right] \end{aligned} \tag{71}$$

and for the $\rho z$-component we have:

$$\frac{t^L_{\rho z}(\mathbf{r})}{F(\zeta)} \approx \left[\frac{\sin\eta\,\cos\eta}{\sinh^2\xi\,\cosh\xi}\right] = \frac{f^3}{r^3}\,\sin\eta\,\cos\eta. \tag{72}$$

From which we get:

$$t^L_{\rho z}(\mathbf{r}) = \frac{1}{\epsilon_m}\frac{3}{4\pi\epsilon_0 r^3}\,\sin\eta\,\cos\eta. \tag{73}$$

It suffices to use that for large distances $\eta = \pi/2 - \theta$, where $\theta$ is the usual polar angle measured from the $z$-axis, to conclude that the ellipsoidal transfer tensor converges to the dipolar transfer tensor, as should be the case.

This work is supported by the National Science Council of Taiwan under Contracts No. NSC-94-2811-M- 009-020 and NSC-94-2112-M-009-037 and by the Ministry of Education of Taiwan under contract no. MOEATU 95W803.

## References


1. O. Stier, M. Grundmann, D. Bimberg, Phys. Rev. B **59**, 5688 (1999)
2. G.W. Bryant, Phys. Rev. B **37**, 8763 (1988)
3. P. Enders, A. Bärwolff, M. Woerner, D. Suisky, Phys. Rev. B **51**, 16695 (1995)
4. J.I. Climente, J. Planelles, W. Jaskolski, Phys. Rev. B **68**, 075307 (2003); J. Climente, J. Planelles, W. Jaskolski et al., J. Phys. C **15**, 3593 (2003)
5. C.M.J. Wijers, Phys. Rev. A **70**, 063807 (2004)
6. O. Voskoboynikov, C.M.J. Wijers, J.L. Liu, C.P. Lee, Phys. Rev. B **71**, 245332 (2005)
7. O. Voskoboynikov, C.M.J. Wijers, J.L. Liu, C.P. Lee, Europhys. Lett. **70**, 656 (2005)
8. C.G. Darwin, Proc. Roy. Soc. of London A **146**, 17 (1934)
9. H.A. Kramers, W. Heisenberg, Z. Phys. **31**, 681 (1925)
10. P. Nozières, D. Pines, Phys. Rev. **109**, 762 (1958)
11. S.L. Adler, Phys. Rev. **126**, 413 (1962)
12. N. Wiser, Phys. Rev. **129**, 62 (1963)
13. C.H. Patterson, D. Weaire, J.F. McGilp, J. of Phys.: Cond. Matt. **4**, 4017 (1992)
14. C.M.J. Wijers, Phys. Stat. Sol. A **188**, 1251 (2001)
15. O. Keller, J. Opt. Soc. Am. B **11**, 1480 (1994)
16. E. Zaremba, B.N.J. Persson, Phys. Rev. B **35**, 596 (1987)
17. J.E. Sipe, J. van Kranendonk, Phys. Rev. A **9**, 1806 (1974)
18. J. Avelin, *Polarizability Analysis of Canonical Dielectric and Bi-anisotropic Scatterers*, Ph.D. thesis, Electromagnetics Laboratory, Helsinki University of Technology, Report 414, 2003.
19. C.M.J. Wijers, G.P.M. Poppe, A. van Silfhout, Phys. Rev. B **44**, 7917 (1991)
20. C.M.J. Wijers, G.P.M. Poppe, Phys. Rev. B **46**, 7605 (1992)
21. J. Vlieger, Physica **64**, 63 (1973); C.M.J. Wijers, K.M.E. Emmett, Physica Scripta **38**, 435 (1988)
22. O. Litzman, P. Rózsa, Surface Science **66**, 542 (1977)
23. S.L. Chuang, *Physics of Optoelectronic Devices* (Wiley, 1995)
24. S. Chandra, S. Tripura Sundari, G. Ravaghan, A.K. Tyagi, J. Phys. D **36**, 2121 (2003)